AGU PUBLICATIONS

Geophysical Research Letters

RESEARCH LETTER
10.1002/2017GL073936

Key Points:
- Antarctic sea ice, buoyancy loss, abyssal stratification, and ocean overturning circulation are related across glacial and modern simulations
- Insufficient sea ice formation and short integration times lead to discrepancies between different glacial climate simulations and paleodata

Supporting Information:
- Supporting Information S1

Correspondence to:
A. Marzocchi,
amarzocchi@uchicago.edu

Citation:
Marzocchi, A., and M. F. Jansen (2017), Connecting Antarctic sea ice to deep-ocean circulation in modern and glacial climate simulations, *Geophys. Res. Lett.*, *44*, 6286–6295, doi:10.1002/2017GL073936.

Received 25 FEB 2017
Accepted 3 JUN 2017
Accepted article online 7 JUN 2017
Published online 17 JUN 2017

Connecting Antarctic sea ice to deep-ocean circulation in modern and glacial climate simulations

Alice Marzocchi[1] **and Malte F. Jansen**[1]

[1]Department of the Geophysical Sciences, The University of Chicago, Chicago, Illinois, USA

Abstract Antarctic sea-ice formation plays a key role in shaping the abyssal overturning circulation and stratification in all ocean basins, by driving surface buoyancy loss through the associated brine rejection. Changes in Antarctic sea ice have therefore been suggested as drivers of major glacial-interglacial ocean circulation rearrangements. Here, the relationship between Antarctic sea ice, buoyancy loss, deep-ocean stratification, and overturning circulation is investigated in Last Glacial Maximum and preindustrial simulations from the Paleoclimate Modelling Intercomparison Project (PMIP). The simulations show substantial intermodel differences in their representation of the glacial deep-ocean state and circulation, which is often at odds with the geological evidence. We argue that these apparent inconsistencies can largely be attributed to differing (and likely insufficient) Antarctic sea-ice formation. Discrepancies can be further amplified by short integration times. Deep-ocean equilibration and sea-ice representation should, therefore, be carefully evaluated in the forthcoming PMIP4 simulations.

1. Introduction

The geological record of the Last Glacial Maximum (LGM, ~21,000 years ago) indicates that lower than modern atmospheric carbon dioxide (CO_2) concentrations resulted in globally cooler air temperatures and extensive ice sheet growth [*Clark and Mix*, 2002], with an equatorward expansion of the sea-ice cover [*Gersonde et al.*, 2005]. The structure of the ocean meridional overturning circulation (MOC) is also thought to have been substantially different; the leading interpretation from geochemical tracers suggests that the volume occupied by Antarctic-sourced water was larger than today, with Antarctic Bottom Water (AABW) spreading across all ocean basins below 2 km, while North Atlantic Deep Water (NADW) was confined to shallower depths [e.g., *Duplessy et al.*, 1988, 2005; *Lynch-Stieglitz et al.*, 2007]. The extent of the shoaling of the upper cell remains, however, uncertain [e.g., *Gebbie*, 2014]. Despite some uncertainties in the reconstructions [e.g., *Miller et al.*, 2015; *Wunsch*, 2016], the abyssal ocean was likely more stratified, with much higher salinities in the Southern Ocean [*Adkins et al.*, 2002]. These glacial-interglacial rearrangements in deep water mass distribution are thought to have contributed to the reduced CO_2 concentrations detected during glacial periods, by affecting the partitioning of carbon between atmosphere and ocean [*Brovkin et al.*, 2007; *Watson et al.*, 2015]. However, we still lack a quantitative understanding of the physical mechanisms leading to the inferred changes, which inevitably challenges our interpretation of past and present climates and shakes our confidence in future projections.

Changes in Antarctic sea ice and the resulting buoyancy forcing have been suggested as drivers of the rearrangements undergone by the Atlantic Meridional Overturning Circulation (AMOC) between glacial and interglacial stages [*Shin et al.*, 2003; *Bouttes et al.*, 2010; *Ferrari et al.*, 2014; *Jansen*, 2017]. In the Southern Ocean, sea-ice formation and the associated brine rejection play a key role in AABW formation, by contributing to the negative buoyancy fluxes around Antarctica [*Marshall and Speer*, 2012; *Talley*, 2013]. As shown by *Jansen and Nadeau* [2016] in idealized ocean-only simulations, enhanced buoyancy loss rates around Antarctica lead to increased abyssal stratification and ultimately a shoaling of NADW. The buoyancy budget of the abyssal overturning cell requires that surface buoyancy loss around Antarctica is balanced by a diffusive buoyancy exchange with the upper cell. For a given diapycnal diffusivity, the diffusive buoyancy flux is directly proportional to the buoyancy gradient at the cell interface, which is well approximated by the vertical stratification. All else being equal, stratification then increases approximatively linearly with the total surface buoyancy loss rate around Antarctica. The stronger abyssal stratification has been argued to ultimately cause a shoaling of the interhemispheric overturning [*Jansen and Nadeau*, 2016]. Building on these theoretical arguments,

Jansen [2017] suggests that glacial-interglacial rearrangements in deep-ocean circulation can be interpreted as a direct consequence of changes in atmospheric temperature. Cooling would lead to more sea-ice formation, which would increase buoyancy loss via brine rejection, resulting in increased stratification and a shallower AMOC [*Jansen and Nadeau*, 2016; *Jansen*, 2017], consistent with the LGM proxy archive.

The attribution of circulation changes to enhanced sea-ice export around Antarctica is consistent with a previous analysis of LGM simulations with the Community Climate System Model (CCSM) [*Shin et al.*, 2003] as well as more recent studies [e.g., *Klockmann et al.*, 2016]. Increased abyssal stratification and a shallower AMOC are also found in the LGM simulation with CCSM3 [*Otto-Bliesner et al.*, 2006], conducted as part of Paleoclimate Modelling Intercomparison Project 2 (PMIP2), where the reproduced ocean circulation best matched the paleoreconstructions compared to other models. However, other PMIP simulations are characterized by substantial discrepancies in their representation of the glacial AMOC, both between different models and with the available data [*Otto-Bliesner et al.*, 2007; *Weber et al.*, 2007; *Muglia and Schmittner*, 2015]. Such inconsistencies cast some doubts on the reliability of these models, which are also used to simulate future climate scenarios.

Here we analyze the relationship between Antarctic sea ice, buoyancy loss, abyssal stratification, and the depth of the AMOC, in climate simulations from the PMIP3 archive [*Braconnot et al.*, 2012], as well as the well-performing CCSM3 (PMIP2) simulation. We also compare these fully-coupled simulations to idealized ocean-only experiments [*Jansen*, 2017] and aim to explain some of the apparent discrepancies between different models and the geological record.

2. Climate Simulations and Analysis

Our analysis is focused on the CCSM3 (PMIP2) [*Otto-Bliesner et al.*, 2006] and CCSM4 (PMIP3) [*Brady et al.*, 2013] preindustrial (PI) control and LGM simulations, which are compared to the other eight PMIP3 models (Table S2 in the supporting information). PMIP3/PMIP2 data and LGM experimental design and boundary conditions are available online (see supporting information). We analyze the monthly 100-year climatologies from the PMIP archive, except for the CCSM4 LGM simulation, where we use an extended simulation [*Brady et al.*, 2013]. This is the only simulation for which time-dependent data from the spin-up phase is available. The idealized simulations used for comparison are described in *Jansen* [2017].

The analyzed PMIP variables are surface air temperature, wind speed and stress, sea-ice concentration, surface heat and freshwater fluxes into sea water, ocean temperature and salinity, and meridional overturning circulation. Note that not all variables are available for all models. Except where stated otherwise, all results are based on annual climatological averages.

Buoyancy loss rates around Antarctica are based on surface heat and freshwater fluxes, and the "integrated buoyancy loss rate" includes all net negative buoyancy fluxes south of the sea-ice line (areas with at least 15% annual mean sea-ice concentration in the Southern Hemisphere), which generally includes all regions of deep-water formation (see Figures 1a and 1b). An exception is the PI simulation with MRI-CGCM3, which has some deep convection outside the sea-ice area; including the buoyancy loss in this region does not significantly modify our results. All buoyancies and potential densities discussed in the paper are referenced to 2000 dbar.

The observational sea-ice extent shown in Figure 3 was calculated by *Roche et al.* [2012] from a compilation of data sets, where the LGM estimates are mainly derived from diatom-based evidence, with large associated uncertainties, especially for the summer months [*Roche et al.*, 2012, and references therein]. Sea-ice extent in the models is defined consistently with the observational estimates, as the area with at least 15% annual mean sea-ice concentration.

3. Last Glacial Maximum and Preindustrial Simulated Climates

PMIP simulations are analyzed in order to test whether the relationship between increased sea-ice formation and buoyancy loss rates, enhanced deep-ocean stratification, and shoaling of the glacial upper overturning cell that is predicted from theory and idealized simulations also operates in the higher-complexity models. We first focus on the CCSM3 and CCSM4 simulations, which show strongly increased sea-ice cover during the LGM; then, results are compared across the PMIP3 ensemble.

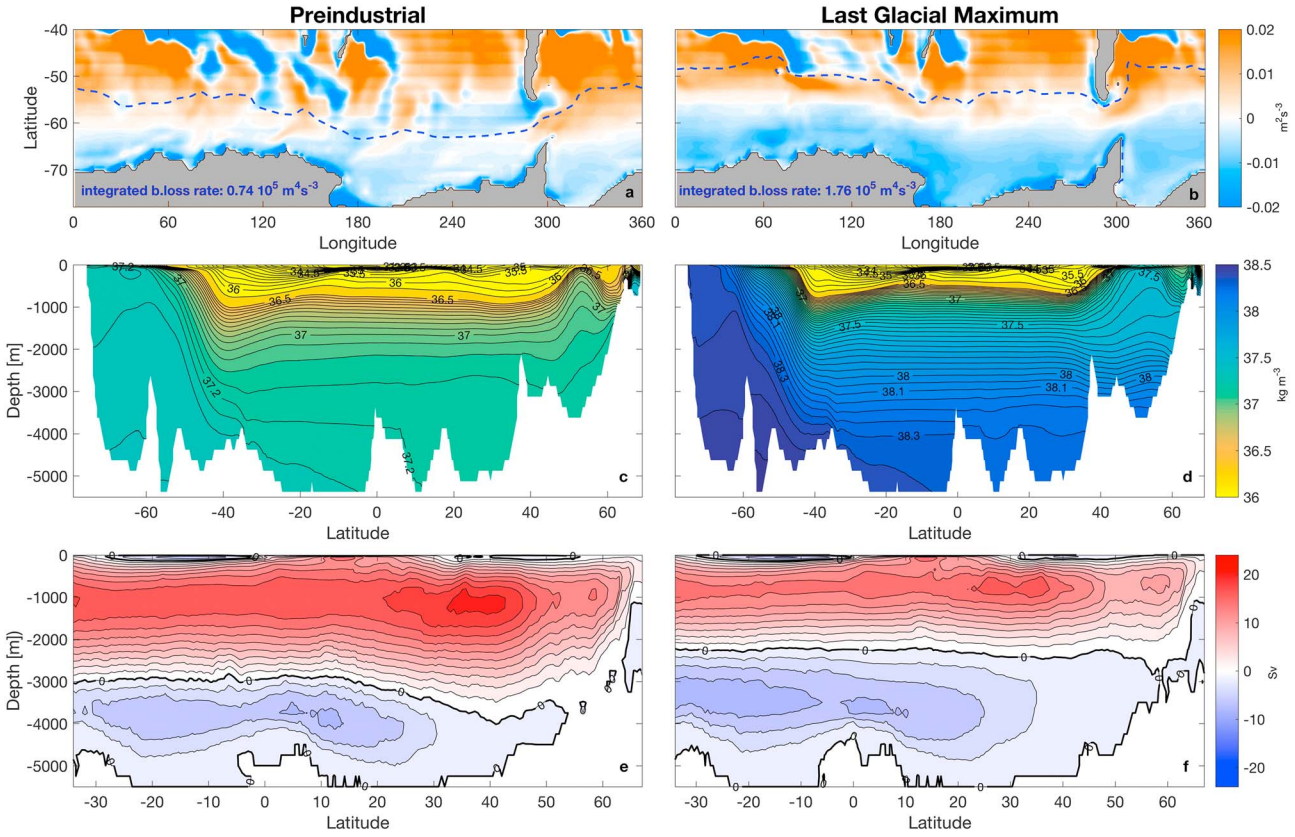

Figure 1. PI (a, c, e) and LGM (b, d, f) CCSM3 simulations. (a, b) Buoyancy fluxes and integrated buoyancy loss rates south of the sea-ice line (dashed blue line; see section 2 for details). (c, d) Potential density for the Atlantic cross section at 26°W (1 g kg^{-1} is subtracted from the LGM salinity). Contour interval: from 0.25 to 0.05 at 36.5 kg^{-1}. (e, f) Atlantic meridional overturning stream function (units of volume transport, where 1 Sverdrup (Sv) = 10^6 m^3 s^{-1}); red colors identify the upper cell and blue the abyssal cell. Contour interval: 2 Sv.

3.1. Ocean Circulation in CCSM3 and CCSM4

The CCSM3 simulation best matches LGM reconstructions. Increased LGM sea ice formation leads to enhanced buoyancy loss around Antarctica (Figures 1a and 1b) [see also *Ferrari et al.*, 2014], which drives increased deep-ocean stratification (Figures 1c and 1d). The stronger stratification is accompanied by a shoaling of the upper overturning cell for the LGM (Figures 1e and 1f), which is consistent with the theoretical arguments in *Jansen and Nadeau* [2016] and *Jansen* [2017]. These results also broadly match the LGM geological record [e.g., *Adkins et al.*, 2002; *Curry and Oppo*, 2005].

Unlike CCSM3, CCSM4 exhibits a strengthening and only limited shoaling of the glacial AMOC (Figure S2f, supporting information), more similar to other PMIP3 models, which mostly show a deepening of the upper cell [*Muglia and Schmittner*, 2015]. The increase in deep-ocean stratification between the PI and LGM simulations is also much less pronounced in CCSM4 as compared to CCSM3 (Figures 1 and S2). Changes in LGM sea-ice concentration and buoyancy loss rates around Antarctica, however, are slightly higher in CCSM4 than in CCSM3 (Figures 1b and S2b). We argue that the comparatively weak LGM stratification and the deep AMOC in CCSM4 can be attributed primarily to a lack of equilibration of the deep-ocean circulation. As shown in Figure 2, the CCSM4 simulation is clearly affected by drifts in deep-ocean temperature and salinity, which result in an ongoing increase in stratification, and a reduction of AMOC depth and strength. Stratification more than doubles during the last 900 integration years, with no obvious slowdown of the trend (Figure 2a). The upper cell shoals by 300–400 m (Figure 2b), while its maximum progressively weakens by about 9 Sv (Figure 2c). As a result, stratification is already significantly strengthened by the end of the extended simulation, as compared to the PMIP3 time slice, and the AMOC becomes shallower and weaker. Notice that no discernible trend can be identified in the maximum AMOC when focusing on the 100-year PMIP period (Figure 2c, dashed grey line), as it is masked by internal variability. Therefore, 100-year AMOC trends are not an adequate metric to determine equilibration.

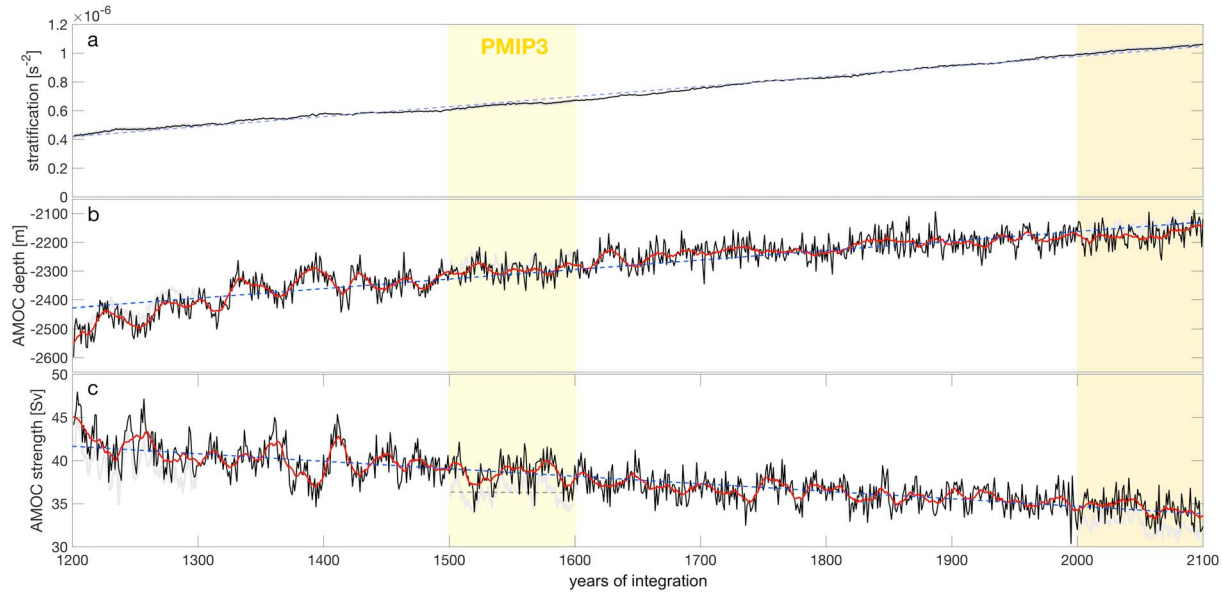

Figure 2. (a) Stratification, (b) AMOC depth, and (c) strength throughout the last 900 years of the CCSM4 LGM simulation, including trends (dashed blue) and running means (solid red). Background shading highlights the PMIP3 climatology (yellow) and the last 100 years of the continuation run (orange) used for analysis. Buoyancy stratification is averaged across the 26°W cross section of Figures 1c and 1d, between 2 and 4 km and between 40°N and 40°S. AMOC strength is defined as the maximum in the overturning stream function, and the depth indicates where this value is reduced by 50%. Years of integration are defined from the PMIP3 spin-up (see supporting information). For computational and storage reasons, data are only shown for the month of June (black), but annual averages (grey) from the beginning, end, and PMIP3 parts of the run show that this does not affect the trends significantly.

3.2. Antarctic Sea Ice Across the PMIP3 Ensemble

LGM sea-ice extent shows a large spread between the PMIP3 models (Figure 3). Importantly, most PMIP3 LGM simulations exhibit a considerably smaller maximum sea ice cover than estimated from the proxy data, even when their PI sea-ice extent is relatively close to observations [see also *Goosse et al.*, 2013]. Only CCSM3 (included for comparison), CCSM4 and MRI-CGCM3 simulate LGM sea-ice extent in closer agreement with the paleoreconstructions (Figure 3) [see also *Sime et al.*, 2016]. Both versions of CCSM stand out for the highest sea-ice cover, in both LGM and PI simulations, although both models overestimate sea-ice extent for the present day [e.g., *Landrum et al.*, 2012]. The overestimated sea-ice cover in the CCSM PI simulations suggests that the large LGM extent may be obtained for the wrong reason. Nevertheless, the simulations allow us to examine the implications of enhanced sea-ice formation on deep-ocean stratification and circulation.

3.3. From Simulated Sea-Ice Changes to a Modified Overturning Circulation

In this subsection, we analyze the relationship between Southern Hemisphere high-latitude surface air temperatures (SAT), Antarctic sea-ice extent, surface buoyancy loss rates, deep-ocean stratification, and AMOC depth, across all PI and LGM simulations.

The PMIP ensemble is characterized by a high negative correlation between SAT and sea-ice extent ($R^2 = 0.87$; Figure 4a), confirming that cold high-latitude temperatures are associated with large sea-ice extent. Notice, however, that unlike in the idealized simulations of *Jansen* [2017], where SAT is prescribed, the causality in the coupled models is less straightforward, as sea ice feeds back on SAT via its effect on surface albedo and atmosphere-ocean heat exchange. Note that all correlations in Figure 4 are significant on a 95% confidence level and that similar (if not higher) correlations are obtained when analyzing LGM-PI anomalies for each model (Figure S5, supporting information).

High positive correlations are also found between sea-ice concentration and buoyancy loss rates ($R^2 = 0.70$; Figure 4b), although the MRI-CGCM3 LGM simulation is an outlier here, with relatively low buoyancy loss rates around Antarctica despite large sea-ice extent (this is discussed further in section 4.1). Notice that buoyancy loss is directly affected by sea-ice formation via brine rejection. Figure 4b relates buoyancy loss rates to sea-ice extent, a relationship that is less obvious but more powerful, as sea-ice cover can more readily be constrained from paleoreconstructions than sea-ice formation rates.

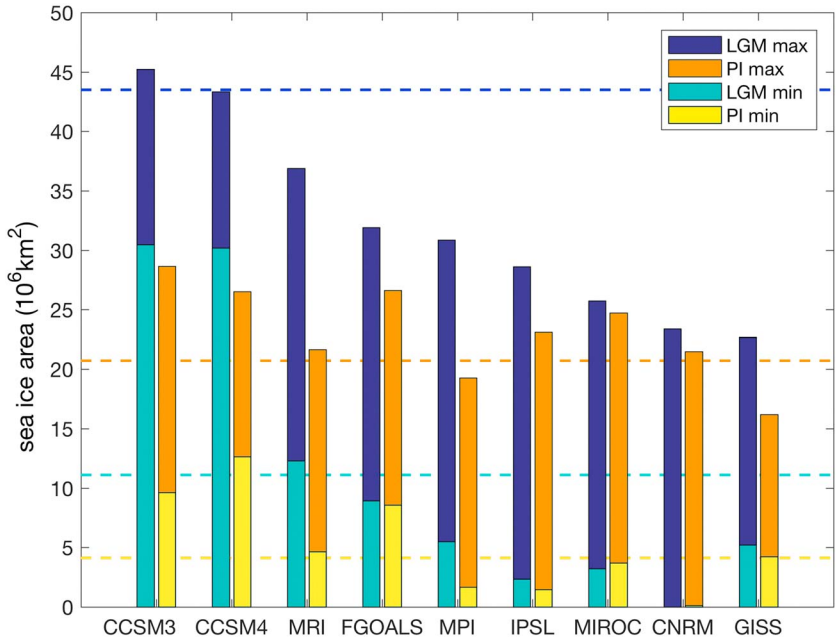

Figure 3. Maximum and minimum Southern Hemisphere sea-ice extent in PI and LGM simulations from the PMIP3 ensemble and CCSM3 (PMIP2); this is equivalent to Figure 1 in *Roche et al.* [2012] for PMIP2 models. The sea-ice-covered area is defined using a 15% sea-ice concentration threshold. Dashed lines are estimates from present-day observations and LGM sea-ice proxies as calculated by *Roche et al.* [2012, and references therein].

The correlation between buoyancy loss rates and stratification is somewhat weaker ($R^2 = 0.54$; Figure 4c), but still highly significant. Notably, all models apart from CCSM3 and CCSM4 show decreased LGM stratification compared to their PI control simulations. While a less stratified deep ocean is in contrast with the LGM proxy record, this does not strongly affect the cross-model correlation between stratification and buoyancy loss, as changes in the buoyancy loss rate between PI and LGM simulations are also small in these models. The CCSM4 LGM simulation is an outlier in Figure 4c, with much weaker stratification than expected based on the large surface buoyancy loss around Antarctica. This behavior is likely to be explained by the still ongoing increase in stratification (Figure 2a). The correlation between buoyancy loss rate and stratification would likely improve if the CCSM4 LGM simulation was integrated for longer. Lack of equilibration may also be an issue in some of the other simulations.

Finally, a significant correlation is found between deep-ocean stratification and AMOC depth ($R^2 = 0.49$; Figure 4d). Most PMIP3 models show a substantially stronger and deeper upper overturning cell in the LGM simulations, as compared to their respective PI controls [see also *Muglia and Schmittner*, 2015]. This is in disagreement with the geological record, but consistent with the relationship between deep-ocean stratification and AMOC depth proposed by *Jansen and Nadeau* [2016], as most of these models also show reduced stratification. Notice, however, that the argument in *Jansen and Nadeau* [2016] assumes that simulations are in equilibrium, which may not be the case for many of the PMIP3 models. The AMOC depth in the LGM simulations may also be affected by wind stress changes in the North Atlantic [*Muglia and Schmittner*, 2015; *Klockmann et al.*, 2016], which is discussed in more detail in section 4.3.

The connection between SAT, buoyancy loss, stratification, and AMOC depth can further be illustrated using a principal component analysis of the five variables across all simulations (Figures 4e and 4f). The first principal component (PC) is characterized by a pattern consistent with our proposed "chain of events," where cold temperatures are associated with large sea-ice extent, high buoyancy loss rates, strong abyssal stratification, and a shallower AMOC (Figure 4e). Different approaches to account for missing data suggest that the dominant pattern is robust and explains more than half of the total variance across simulations (see SI for details on the methodology). The second PC explains much less variance and is unlikely to provide much physical insight (see also Figure S1).

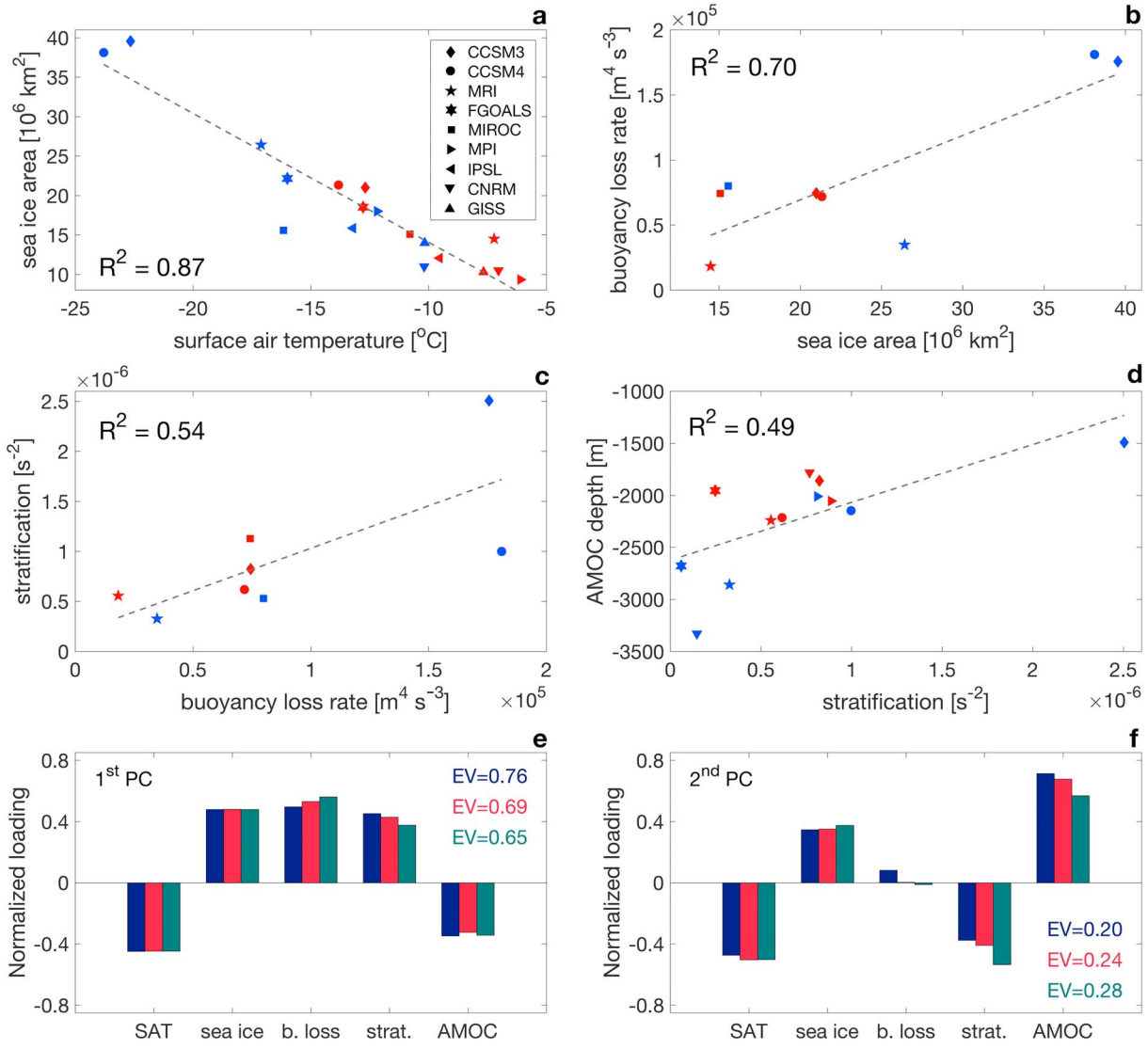

Figure 4. Correlations across all PI (red) and LGM (blue) simulations, between (a) SAT and Antarctic sea ice extent, (b) sea-ice and integrated buoyancy loss rates, (c) buoyancy loss and deep-ocean stratification, and (d) stratification and AMOC depth. The bottom panels show the (e) first and (f) second principal component and their respective explained variance (EV). Note that not all variables exist for all models. Different colors in Figures 4e and 4f represent different methods to account for missing data (see supporting information).

4. Discussion

This study set out to investigate whether the proposed link between Antarctic sea ice expansion and water mass reorganization during glacial times can be verified in LGM climate simulations from the PMIP3 ensemble. A connection between Antarctic sea ice, buoyancy loss, deep-ocean stratification, and a shallower AMOC has previously been identified in idealized simulations [*Jansen*, 2017] and is also broadly consistent with a number of more complex coupled simulations of glacial climates [*Shin et al.*, 2003; *Liu et al.*, 2005; *Klockmann et al.*, 2016; *Sun et al.*, 2016], including the CCSM3 LGM simulation (section 3.1 and Figures 1 and 4). The analysis in section 3.3 suggests that the relationship between the variables in question largely holds true over a broader ensemble of models. However, most of the PMIP3 LGM simulations do not show an increase in abyssal stratification and shoaling of the AMOC compared to their PI control experiments, in contrast with the proxy record. As further discussed in the following subsections, our analysis can largely attribute these apparent inconsistencies to insufficient sea-ice formation and export (section 4.1) and the lack of deep-ocean equilibrium (section 4.2), although additional changes in the forcing are also likely to play a significant role (section 4.3).

4.1. Sea-Ice Formation and Export

Given the substantial differences in LGM Antarctic sea ice across the PMIP3 models (Figure 3), very different feedbacks on ocean circulation are to be expected. Simulations showing little or no sea-ice increase typically reveal circulation patterns opposite to those inferred from proxy reconstructions. Models simulating large LGM sea-ice extent instead exhibit changes in circulation and stratification that are largely consistent with the proxy record and the hypothesized theoretical argument. One obvious exception is MRI-CGCM3.

Despite the good agreement with PI and LGM Antarctic sea-ice extent estimates, MRI does not simulate large LGM surface buoyancy loss, unlike the CCSM simulations (Figure 4b). The reason for this appears to be a virtually complete vanishing of wind stress over sea-ice-covered regions (Figure S4, supporting information), which inhibits sea-ice export and thus brine rejection associated with new sea-ice formation. Following the theoretical argument, enhanced Antarctic buoyancy loss from brine rejection is a prerequisite for both enhanced abyssal stratification and a shallower AMOC; it is, therefore, unsurprising that neither of these are found in the MRI LGM simulation (Figures 4c and 4d). The near-disappearance of wind stress over sea ice is the result of a model bug in MRI (S. Murakami, personal communication, 2017). The lack of wind stress (and thus frictional drag) over sea ice in MRI is also likely to explain why this model is an outlier in several LGM studies focused on changes in the wind fields [*Chavaillaz et al.*, 2013; *Rojas*, 2013; *Liu et al.*, 2015; *Sime et al.*, 2016].

Model biases in the representation of sea ice and buoyancy fluxes may also be linked to Antarctic polynyas. Polynyas were likely active at the LGM [e.g., *Smith et al.*, 2010; *Weber et al.*, 2011] but are often simulated unrealistically in coupled models, which can results in erroneous representations of deep convection and AABW formation [e.g., *Stössel et al.*, 2002; *Kerr et al.*, 2009; *Heuzé et al.*, 2013].

4.2. Deep-Ocean Equilibration and Transient AMOC Response

Time series data (Figure 2) clearly show that the CCSM4 LGM simulation has not yet equilibrated and that the equilibrium solution would most likely have a higher abyssal stratification, as well as a shallower AMOC. The lack of equilibration is likely to explain much, if not most, of the difference between the LGM ocean states in CCSM4 and CCSM3. Notice that the CCSM3 LGM integration is much shorter than CCSM4 and is not equilibrated either [*Brandefelt and Otto-Bliesner*, 2009] but appears to be closer to its equilibrium solution, likely helped by the fact that the run was initialized from an existing LGM simulation.

During its spin-up, the CCSM4 LGM simulation is characterized by an initial deepening and substantial strengthening of the AMOC, which gets progressively shallower and weaker throughout the run (Figures 2 and S3). A similar transient response to surface cooling is found in idealized ocean-only simulations, where the AMOC adjusts nonmonotonically, exhibiting a strong initial "overshoot" of the upper cell, before eventually shoaling (Figure S3). A similar behavior may also affect other PMIP3 models, which would contribute to an unrealistically strong and deep AMOC in nonequilibrated LGM simulations that are spun up from PI initial conditions. Especially at risk are simulations with very short integration times, such as the FGOALS-g2 LGM run, which exhibits a very strong and deep AMOC but was run for no longer than 800 years in total [*Zheng and Yu*, 2013]. However, we were only able to quantify the role of transient adjustment in CCSM4, as time-dependent data are not available in the PMIP3 archive, and attempts to obtain additional output were successful only for this model.

Potential issues associated with a lack of equilibration in LGM simulations have been highlighted previously [e.g., *Brandefelt and Otto-Bliesner*, 2009; *Zhang et al.*, 2013] and stress the importance to carefully assess deep-ocean equilibrium in future PMIP simulations. Notice that the CCSM4 LGM simulation does not have a particularly large global surface ocean heat flux imbalance (about 0.8 W m^{-2}, an average value even for PI simulations; e.g. *Lucarini and Ragone* [2011]), suggesting that the net ocean heat budget alone may not be a good indicator for deep-ocean equilibration. The equilibrium timescale for the deep ocean has been shown to depend strongly on the initial conditions [*Zhang et al.*, 2013], emphasizing the potential advantages of spinning up LGM simulations from cold climate states.

4.3. Compensating Feedbacks and Other Forcing

The proposed mechanism analyzed in this study appears to explain about half of the variance in sea ice, buoyancy loss, stratification and AMOC depth across simulations (Figure 4). While somewhat higher explained variances may be expected if all simulations were integrated to equilibrium, additional mechanisms are likely to be responsible for some of the models' spread.

Muglia and Schmittner [2015] attribute the deeper and stronger AMOC found in most PMIP3 simulations to the effect of stronger westerlies over the North Atlantic, which in turn are linked to the modified height of the Northern Hemisphere ice sheets in the PMIP3 boundary conditions. *Klockmann et al.* [2016] recently showed that both the Antarctic buoyancy loss mechanism discussed here, as well as the wind stress effect discussed by *Muglia and Schmittner* [2015], appear to be active in MPI-ESM, where they compensate almost entirely, leading to very little changes in the simulated AMOC between LGM and PI simulations. A similar compensating effect may be present in other PMIP3 models, as well as in the PMIP2 ensemble, where the intermodel spread was even larger [e.g., *Otto-Bliesner et al.*, 2007].

Several other mechanisms have been suggested to explain glacial-interglacial ocean circulation differences, including changes in the strength and position of the Southern Ocean westerly winds [e.g., *Toggweiler et al.*, 2006; *Tschumi et al.*, 2008], and changes in tidal mixing during glacial climates [*Wunsch*, 2003; *Schmittner et al.*, 2015]. Recent observational and modeling studies, however, indicate that changes in the westerlies are unlikely to be as large or relevant as previously suggested [*Kohfeld et al.*, 2013; *Rojas*, 2013; *Völker and Köhler*, 2013; *Sime et al.*, 2016]. Increased tidal mixing may partly counteract the effects of increased buoyancy loss around Antarctica [see also *Jansen*, 2017] but this cannot be verified in the PMIP3 simulations, which do not account for stronger LGM tidal mixing.

5. Summary and Conclusions

The relationship between Antarctic sea ice, deep-ocean stratification, and overturning circulation is analyzed in climate simulations from the CMIP/PMIP archive. Discrepancies in the simulated stratification and circulation between different LGM simulations are shown to be related to Antarctic sea-ice formation and export. Models simulating large sea-ice formation also exhibit strong deep-ocean stratification and a shallower AMOC, consistent with the geological record. LGM simulations with relatively little Antarctic sea ice, instead typically reveal stratification and circulation changes opposite to those inferred from proxy reconstructions. In simulations where differences in Antarctic sea ice extent between PI and LGM are relatively small, AMOC changes may be dominated by increased wind stress in the North Atlantic, which tends to favor a deepening and strengthening of the overturning [*Muglia and Schmittner*, 2015; *Klockmann et al.*, 2016], at odds with the proxy evidence for this time period. Discrepancies between models and paleodata can be further amplified by short integration times, as the transient response to cooling is expected to be associated with a stronger and deeper AMOC. The need to carefully evaluate deep-ocean equilibration should, therefore, be taken into account in the planning of the forthcoming PMIP4 simulations [e.g., *Ivanović et al.*, 2016]. While it is expected that not all simulations in the archive can be integrated to full equilibrium, the level of deep-ocean equilibration should be clarified and, if possible, time series data from the spin-up should be provided to allow for a quantitative evaluation and avoid erroneous interpretations.

Acknowledgments
We thank Ruza Ivanovic, the Editor, and three anonymous reviewers for valuable comments and the modeling groups participating in PMIP for making their model output available. Links to the PMIP data repositories are provided in the SI; data from the idealized simulations can be obtained from MFJ (e-mail: mfj@uchicago.edu). This work was funded by the National Science Foundation under award 1536454.

References

Adkins, J. F., K. McIntyre, and D. P. Schrag (2002), The salinity, temperature, and δ^{18}O of the glacial deep ocean, *Science*, *298*(5599), 1769–1773, doi:10.1126/science.1076252.

Bouttes, N., D. Paillard, and D. M. Roche (2010), Impact of brine-induced stratification on the glacial carbon cycle, *Clim. Past*, *6*(5), 575–589, doi:10.5194/cp-6-575-2010.

Braconnot, P., S. P. Harrison, M. Kageyama, P. J. Bartlein, V. Masson-Delmotte, A. Abe-Ouchi, B. Otto-Bliesner, and Y. Zhao (2012), Evaluation of climate models using palaeoclimatic data, *Nat. Clim. Change*, *2*(6), 417–424, doi:10.1038/nclimate1456.

Brady, E. C., B. L. Otto-Bliesner, J. E. Kay, and N. Rosenbloom (2013), Sensitivity to glacial forcing in the CCSM4, *J. Clim.*, *26*(6), 1901–1925, doi:10.1175/JCLI-D-11-00416.1.

Brandefelt, J., and B. L. Otto-Bliesner (2009), Equilibration and variability in a Last Glacial Maximum climate simulation with CCSM3, *Geophys. Res. Lett.*, *36*, L19712, doi:10.1029/2009GL040364.

Brovkin, V., A. Ganopolski, D. Archer, and S. Rahmstorf (2007), Lowering of glacial atmospheric CO_2 in response to changes in oceanic circulation and marine biogeochemistry, *Paleoceanography*, *22*, PA4202, doi:10.1029/2006PA001380.

Chavaillaz, Y., F. Codron, and M. Kageyama (2013), Southern westerlies in LGM and future (RCP4.5) climates, *Clim. Past*, *9*(2), 517–524, doi:10.5194/cp-9-517-2013.

Clark, P. U., and A. C. Mix (2002), Ice sheets and sea level of the Last Glacial Maximum, *Quat. Sci. Rev.*, *21*(1–3), 1–7, doi:10.1016/S0277-3791(01)00118-4.

Curry, W. B., and D. W. Oppo (2005), Glacial water mass geometry and the distribution of δ13C of ΣCO_2 in the western Atlantic Ocean, *Paleoceanography*, *20*, PA1017, doi:10.1029/2004PA001021.

Duplessy, J. C., N. J. Shackleton, R. G. Fairbanks, L. Labeyrie, D. Oppo, and N. Kallel (1988), Deepwater source variations during the last climatic cycle and their impact on the global deepwater circulation, *Paleoceanography*, *3*(3), 343–360, doi:10.1029/PA003i003p00343.

Ferrari, R., M. F. Jansen, J. F. Adkins, A. Burke, A. L. Stewart, and A. F. Thompson (2014), Antarctic sea ice control on ocean circulation in present and glacial climates, *Proc. Natl. Acad. Sci.*, *111*(24), 8753–8758, doi:10.1073/pnas.1323922111.

Gebbie, G. (2014), How much did Glacial North Atlantic Water shoal?, *Paleoceanography*, *29*, 190–209, doi:10.1002/2013PA002557.

Gersonde, R., X. Crosta, A. Abelmann, and L. Armand (2005), Sea-surface temperature and sea ice distribution of the Southern Ocean at the EPILOG Last Glacial Maximum—A circum-Antarctic view based on siliceous microfossil records, *Quat. Sci. Rev.*, *24*(7–9), 869–896, doi:10.1016/j.quascirev.2004.07.015.

Goosse, H., D. M. Roche, A. Mairesse, and M. Berger (2013), Modelling past sea ice changes, *Quat. Sci. Rev.*, *79*, 191–206, doi:10.1016/j.quascirev.2013.03.011.

Heuzé, C., K. J. Heywood, D. P. Stevens, and J. K. Ridley (2013), Southern ocean bottom water characteristics in CMIP5 models, *Geophys. Res. Lett.*, *40*, 1409–1414, doi:10.1002/grl.50287.

Ivanović, R. F., L. J. Gregoire, M. Kageyama, D. M. Roche, P. J. Valdes, A. Burke, R. Drummond, W. R. Peltier, and L. Tarasov (2016), Transient climate simulations of the deglaciation 21–9 thousand years before present (version 1)—PMIP4 Core experiment design and boundary conditions, *Geosci. Model Dev.*, *9*(7), 2563–2587, doi:10.5194/gmd-9-2563-2016.

Jansen, M. F. (2017), Glacial ocean circulation and stratification explained by reduced atmospheric temperature, *Proc. Natl. Acad. Sci. U.S.A.*, *114*(1), 45–50, doi:10.1073/pnas.1610438113.

Jansen, M. F., and L.-P. Nadeau (2016), The effect of Southern Ocean surface buoyancy loss on the deep-ocean circulation and stratification, *J. Phys. Oceanogr.*, *46*(11), 3455–3470, doi:10.1175/JPO-D-16-0084.1.

Kerr, R., I. Wainer, and M. M. Mata (2009), Representation of the Weddell Sea deep water masses in the ocean component of the NCAR-CCSM model, *Antarct. Sci.*, *21*(3), 301–312, doi:10.1017/S0954102009001825.

Klockmann, M., U. Mikolajewicz, and J. Marotzke (2016), The effect of greenhouse gas concentrations and ice sheets on the glacial AMOC in a coupled climate model, *Clim. Past*, *12*(9), 1829–1846, doi:10.5194/cp-12-1829-2016.

Kohfeld, K. E., R. M. Graham, A. M. de Boer, L. C. Sime, E. W. Wolff, C. Le Quéré, and L. Bopp (2013), Southern Hemisphere westerly wind changes during the Last Glacial Maximum: Paleo-data synthesis, *Quat. Sci. Rev.*, *68*, 76–95, doi:10.1016/j.quascirev.2013.01.017.

Landrum, L., M. M. Holland, D. P. Schneider, and E. Hunke (2012), Antarctic sea ice climatology, variability, and late twentieth-century change in CCSM4, *J. Clim.*, *25*(14), 4817–4838, doi:10.1175/JCLI-D-11-00289.1.

Liu, W., J. Lu, L. R. Leung, S.-P. Xie, Z. Liu, and J. Zhu (2015), The de-correlation of westerly winds and westerly-wind stress over the Southern Ocean during the Last Glacial Maximum, *Clim. Dyn.*, *45*(11–12), 3157–3168, doi:10.1007/s00382-015-2530-4.

Liu, Z., S.-I. Shin, R. S. Webb, W. Lewis, and B. L. Otto-Bliesner (2005), Atmospheric CO_2 forcing on glacial thermohaline circulation and climate, *Geophys. Res. Lett.*, *32*, L02706, doi:10.1029/2004GL021929.

Lucarini, V., and F. Ragone (2011), Energetics of climate models: Net energy balance and meridional enthalpy transport, *Rev. Geophys.*, *49*, RG1001, doi:10.1029/2009RG000323.

Lynch-Stieglitz, J., et al. (2007), Atlantic meridional overturning circulation during the Last Glacial Maximum, *Science*, *316*(5821), 66–69, doi:10.1126/science.1137127.

Marshall, J., and K. Speer (2012), Closure of the meridional overturning circulation through Southern Ocean upwelling, *Nat. Geosci.*, *5*(3), 171–180, doi:10.1038/ngeo1391.

Miller, M. D., M. Simons, J. F. Adkins, and S. E. Minson (2015), The information content of pore fluid $\delta^{18}O$ and $[Cl^-]$, *J. Phys. Oceanogr.*, *45*(8), 2070–2094, doi:10.1175/JPO-D-14-0203.1.

Muglia, J., and A. Schmittner (2015), Glacial Atlantic overturning increased by wind stress in climate models, *Geophys. Res. Lett.*, *42*, 9862–9868, doi:10.1002/2015GL064583.

Otto-Bliesner, B. L., E. C. Brady, G. Clauzet, R. Tomas, S. Levis, and Z. Kothavala (2006), Last Glacial Maximum and Holocene climate in CCSM3, *J. Clim.*, *19*(11), 2526–2544, doi:10.1175/JCLI3748.1.

Otto-Bliesner, B. L., C. D. Hewitt, T. M. Marchitto, E. Brady, A. Abe-Ouchi, M. Crucifix, S. Murakami, and S. L. Weber (2007), Last Glacial Maximum ocean thermohaline circulation: PMIP2 model intercomparisons and data constraints, *Geophys. Res. Lett.*, *34*, L12706, doi:10.1029/2007GL029475.

Roche, D. M., X. Crosta, and H. Renssen (2012), Evaluating Southern Ocean sea-ice for the Last Glacial Maximum and pre-industrial climates: PMIP-2 models and data evidence, *Quat. Sci. Rev.*, *56*, 99–106, doi:10.1016/j.quascirev.2012.09.020.

Rojas, M. (2013), Sensitivity of Southern Hemisphere circulation to LGM and 4×CO_2 climates, *Geophys. Res. Lett.*, *40*, 965–970, doi:10.1002/grl.50195.

Schmittner, A., J. A. M. Green, and S.-B. Wilmes (2015), Glacial ocean overturning intensified by tidal mixing in a global circulation model, *Geophys. Res. Lett.*, *42*, 4014–4022, doi:10.1002/2015GL063561.

Shin, S.-I., Z. Liu, B. Otto-Bliesner, E. Brady, J. Kutzbach, and S. Harrison (2003), A Simulation of the Last Glacial Maximum climate using the NCAR-CCSM, *Clim. Dyn.*, *20*(2–3), 127–151, doi:10.1007/s00382-002-0260-x.

Sime, L. C., D. Hodgson, T. J. Bracegirdle, C. Allen, B. Perren, S. Roberts, and A. M. de Boer (2016), Sea ice led to poleward-shifted winds at the Last Glacial Maximum: The influence of state dependency on CMIP5 and PMIP3 models, *Clim. Past*, *12*(12), 2241–2253, doi:10.5194/cp-12-2241-2016.

Smith, J. A., C.-D. Hillenbrand, C. J. Pudsey, C. S. Allen, and A. G. Graham (2010), The presence of polynyas in the Weddell Sea during the last glacial period with implications for the reconstruction of sea-ice limits and ice sheet history, *Earth Planet. Sci. Lett.*, *296*(3–4), 287–298, doi:10.1016/j.epsl.2010.05.008.

Stössel, A., K. Yang, and S.-J. Kim (2002), On the role of sea ice and convection in a global ocean model, *J. Phys. Oceanogr.*, *32*(4), 1194–1208, doi:10.1175/1520-0485(2002)032<1194:OTROSI>2.0.CO;2.

Sun, S., I. Eisenman, and A. L. Stewart (2016), The influence of Southern Ocean surface buoyancy forcing on glacial-interglacial changes in the global deep ocean stratification, *Geophys. Res. Lett.*, *43*, 8124–8132, doi:10.1002/2016GL070058.

Talley, L. D. (2013), Closure of the global overturning circulation through the Indian, Pacific, and Southern Oceans: Schematics and transports, *Oceanography*, *26*(1), 80–97.

Toggweiler, J. R., J. L. Russell, and S. R. Carson (2006), Midlatitude westerlies, atmospheric CO_2, and climate change during the ice ages, *Paleoceanography*, *21*, PA2005, doi:10.1029/2005PA001154.

Tschumi, T., F. Joos, and P. Parekh (2008), How important are Southern Hemisphere wind changes for low glacial carbon dioxide? A model study, *Paleoceanography*, *23*, PA4208, doi:10.1029/2008PA001592.

Völker, C., and P. Köhler (2013), Responses of ocean circulation and carbon cycle to changes in the position of the Southern Hemisphere westerlies at Last Glacial Maximum, *Paleoceanography*, *28*, 726–739, doi:10.1002/2013PA002556.

Watson, A. J., G. K. Vallis, and M. Nikurashin (2015), Southern Ocean buoyancy forcing of ocean ventilation and glacial atmospheric CO_2, *Nat. Geosci.*, *8*(11), 861–864, doi:10.1038/ngeo2538.

Weber, M. E., P. U. Clark, W. Ricken, J. X. Mitrovica, S. W. Hostetler, and G. Kuhn (2011), Interhemispheric ice-sheet synchronicity during the Last Glacial Maximum, *Science*, *334*(6060), 1265–1269, doi:10.1126/science.1209299.

Weber, S. L., S. S. Drijfhout, A. Abe-Ouchi, M. Crucifix, M. Eby, A. Ganopolski, S. Murakami, B. Otto-Bliesner, and W. R. Peltier (2007), The modern and glacial overturning circulation in the Atlantic ocean in PMIP coupled model simulations, *Clim. Past*, *3*(1), 51–64, doi:10.5194/cp-3-51-2007.

Wunsch, C. (2003), Determining paleoceanographic circulations, with emphasis on the Last Glacial Maximum, *Quat. Sci. Rev.*, *22*(2–4), 371–385, doi:10.1016/S0277-3791(02)00177-4.

Wunsch, C. (2016), Pore fluids and the LGM ocean salinity-reconsidered, *Quat. Sci. Rev.*, *135*, 154–170, doi:10.1016/j.quascirev.2016.01.015.

Zhang, X., G. Lohmann, G. Knorr, and X. Xu (2013), Different ocean states and transient characteristics in Last Glacial Maximum simulations and implications for deglaciation, *Clim. Past*, *9*(5), 2319–2333, doi:10.5194/cp-9-2319-2013.

Zheng, W., and Y. Yu (2013), Paleoclimate simulations of the mid-Holocene and Last Glacial Maximum by FGOALS, *Adv. Atmos. Sci.*, *30*(3), 684–698, doi:10.1007/s00376-012-2177-6.